Chung Yuan Journal
Vol. 28, No. 3, 2000, pp. 15-22

A Multicomponent Flow Calculation Using MUSCL Type Central Scheme

TIEN-YU SUN AND CHEN-TZU HSU

Department of Mathematics
Chung Yuan Christian University
Chung-Li, 32023, Taiwan, R.O.C.

(Received: May 12, 2000; Accepted: September 6, 2000)

ABSTRACT

In this paper, we demonstrate that we can exploit the Riemann-solver-free feature of MUSCL type central scheme and apply it to single-component and multicomponent one-dimensional, unsteady compressible Euler equations with stiffened gas equation of state. Under the present framework, the traditional difficulty of constructing a proper Riemann solver according to the equation of state considered in multicomponent flow calculation is now eliminated.

Key words: *Compressible Euler equations, multicomponent flow, MUSCL type central scheme, Riemann solver, stiffened gas equation of state.*

I. Introduction

In the past two decades, advances on high resolution methods for solving hyperbolic conservation laws numerically has been very remarkable. The resolution of single-component compressible Euler equations with the polytropic gas equation of state is now a standard topic in a large number of textbooks on computational fluid dynamics. However generalization and application of existing results to single-component compressible Euler equations and to multicomponent compressible Euler equations with more general equation of states are proved to be much more difficult. See [1, 5, 6, 9, 10, 11, 14] for recent development in this direction. One major difficulty is the construction of a proper Riemann solver according to the equation of state considered may be very complicated. Furthermore, it is now well known that, in the computation of multicomponent flows, special care has to be taken on updating the pressure field. Typically, spurious oscillations in pressure appear near interfaces separating the two gases once the time evolution is started and keep growing afterwards. See references listed above for more details.

Recently, progress has been made on the development of Riemann-solver-free central schemes for hyperbolic conservation laws. See [4, 8, 15]. Since characteristic decomposition is no longer performed at each cell interface, central schemes execute significantly faster than traditional Riemann-solver-based methods. Their Riemann-solver-free feature also give them great flexibility so that they are good solvers to be considered in a wide range of applications. However central schemes are usually more diffusive as compared to most Riemann-solver-based methods, especially on the resolution of contact discontinuities. See [4, 8, 12, 14] for numerical tests on central schemes.

The purpose of this paper is to exploit the Riemann-solver-free feature of Toro's MUSCL type central scheme in solving one-dimensional compressible Euler equations of one or more components. In §2, we demonstrate that MUSCL type central scheme can be used to resolve single-component flows of polytropic gases and stiffened gases by making minor changes in the program codes. As a preliminary step in developing a multicoponent alogrithm based on MUSCL type central scheme, a central scheme for solving variable coefficient advection equation is proposed and tested in §3. Then, in §4, an algorithm for resolving multicomponent flows of stiffened gases is given based on the volume-fraction model discussed in great details by Shyue in [10]. Numerical tests given in §4 show that the method of this paper provides an easy to use solver in additional to those Riemann-solver-based methods developed by Saurel, Abgrall and Shyue in [9, 10].

II. One-dimensional MUSCL type central schemes

A. Numerical schemes

To make the paper self-contained, we now give a brief review of the one-dimensional MUSCL type central scheme. Given mesh sizes Δx and time step Δt, we will use the notations x_j and t_n to represent the grid $j\Delta x$ and the time $n\Delta t$. The cell average of $U(x, t)$ over the cell $[x_{j-1/2}, x_{j+1/2}]$ at time t_n is denoted as U_j^n.

Consider the initial value problem of the one-dimensional hyperbolic conservation law

$$U_t + F(U)_x = 0$$

$$U(x, 0) = U_0(x). \tag{2.1}$$

The MUSCL type central scheme has the same framework as the MUSCL-Hancock scheme treated in the most textbooks, such as [13]. First, as a higher resolution extension to the Godunov method, we replace the piecewise constant function

$$U^n(x) = U_j^n, \qquad x \in (x_{j-1/2}, x_{j+1/2})$$

with the piecewise linear function

$$U^n(x) = U_j(x) = U_j^n + \frac{x - x_j}{\Delta x}\Delta_j, \qquad x \in (x_{j-1/2}, x_{j+1/2}). \tag{2.2}$$

Here Δ_j is a slope vector, such as

$$\Delta_j = \frac{1}{2}(U_{j+1} - U_{j-1}).$$

Second, at the boundaries of the cell $[x_{j-1/2}, x_{j+1/2}]$, the boundary extrapolated values $U_j^{\pm}$ are set equal to

$$U_j^- = U_j^n - \frac{1}{2}\Delta_j,$$

$$U_j^+ = U_j^n + \frac{1}{2}\Delta_j, \tag{2.3}$$

Then $U_j^{\pm}$ are evolved by half a time step with

$$\bar{U}_j^+ = U_j^+ - \frac{\Delta t}{2\Delta x}(F(U_j^+) - F(U_j^-)),$$

$$\bar{U}_j^- = U_j^- - \frac{\Delta t}{2\Delta x}(F(U_j^+) - F(U_j^-)). \tag{2.4}$$

The numerical flux $F_{j+1/2}$ of Riemann-solver based MUSCL-Hancock scheme is defined as

$$F_{j+1/2} = F(U_{j+1/2}(0)) \tag{2.5}$$

where $U_{j+1/2}(x/t)$ is the solution of the Riemann problem of (2.1) with Riemann data $(\bar{U}_j^+, \bar{U}_{j+1}^-)$. In MUSCL type central scheme, to avoid the use of Riemann solver, the numerical flux is set equal to

$$F_{j+1/2}^C = F^{force}(\bar{U}_j^+, \bar{U}_{j+1}^-) \tag{2.6}$$

$$= \frac{1}{2}(F^{RI}(\bar{U}_j^+, \bar{U}_{j+1}^-) + F^{LF}(\bar{U}_j^+, \bar{U}_{j+1}^-)), \tag{2.7}$$

where F^{RI} and F^{LF} are the Richtmyer and Lax-Friedrichs fluxes respectively. We have

$$F^{RI}(U^L, U^R) = F(U^{RI}),$$

$$U^{RI} = \frac{1}{2}(U^L + U^R) + \frac{1}{2}\frac{\Delta t}{\Delta x}(F(U^L) - F(U^R)), \tag{2.8}$$

$$F^{LF}(U^L, U^R) = \frac{1}{2}(F(U^L) + F(U^R)) + \frac{1}{2}\frac{\Delta x}{\Delta t}(U^L - U^R).$$

The flux function F^{force} is the numerical flux of the first order FORCE scheme. Then the MUSCL type central scheme gives

$$U_j^{n+1} = U_j^n - \frac{\Delta t}{\Delta x}(F_{j+1/2}^C - F_{j-1/2}^C) \tag{2.9}$$

To suppress spurious oscillations in the numerical solutions, we may replace the slope vector Δ_j in (2.2) with a limited slope vector $\bar{\Delta}_j$. See [12, 13] for possible choices of limited slope vectors Δ_j. In the numerical tests that follow, we will use the UNO limited slope vector, which has the form

$$\bar{\Delta}_j = MM(\Delta_{j-1/2}u + \frac{1}{2}MM(\Delta^2 u_{j-1}\Delta^2 u_j), \Delta_{j+1/2}u - \frac{1}{2}MM(\Delta^2 u_j \Delta^2 u_{j+1})), \tag{2.10}$$

where

$\Delta_{j+1/2}u = u_{j+1} - u_j$,
$\Delta^2 u_j = u_{j+1} - 2u_j + u_{j-1}$,
$MM(u_1, u_2, \ldots)$

$$= \begin{cases} \min_j\{u_j\}, & \text{if } u_j > 0 \text{ for all } j, \\ \max_j\{u_j\}, & \text{if } u_j < 0 \text{ for all } j, \\ 0, & \text{otherwise.} \end{cases}$$

B. Numerical tests

Example 2.1 We begin by considering the one-dimensonal, unsteady Euler equations

$$\frac{\partial}{\partial t}\begin{pmatrix}\rho\\ \rho u\\ E\end{pmatrix}+\frac{\partial}{\partial x}\begin{pmatrix}\rho u\\ \rho u^2+p\\ u(E+p)\end{pmatrix}=0 \tag{2.11}$$

with the polytropic gas equation of state

$$\rho e=\frac{p}{\gamma-1}. \tag{2.12}$$

In (2.11), ρ, u and p are the density, velocity and pressure respectively. $E = \rho u^2/2 + \rho e$ is the total energy where e is the internal energy per unit mass. The coefficient γ is the usual ratio of specific heats. The first test problem is the modified Sod's problem taken from [13], with initial data

$$(\rho, u, p) = (1, 0, 1),\ x<0.4,$$

$$(\rho, u, p) = (0.125, 0, 0.1),\ x>0.4.$$

In (2.12), γ is set equal to 1.4. The computational domain [0, 1] is divided into 100 cells with nonreflecting boundary conditions applied at both end. The time step Δt is chosen by

$$\Delta t = C_{cfl}\frac{\Delta x}{S_{\max}} \tag{2.13}$$

where C_{cfl} is the CFL number. In (2.13),

$$S_{\max}=\max_j(|U_j^n|+a_j^n),$$

where a is the sound speed; $a^2 = \gamma p/\rho$. We set $C_{cfl} = 0.8$. At $t = 0.2$, the resulting profiles of density, velocity and pressure are displayed in Figure 1 below.

Figure 1 indicates that the result generated by MUSCL type central scheme, as compared to numerical results in [13] on the present test problem generated by various methods, is significantly better than first order ones. However the MUSCL type central scheme is still inferior to most high resolution Riemann-solver-based methods used nowadays and is more diffusive near contact discontinuities, as can be seen in Figure 1 near $x = 0.5$. One major advantage of using central schemes is that the process of characteristic decomposition is no longer performed at each cell interface. Thus the matter of designing appropriate Riemann solvers for each fluid in the two phase flow computation can be avoided totally. This flexibility of central schemes can be found in the following example.

Example 2.2 We now consider the Euler equations with

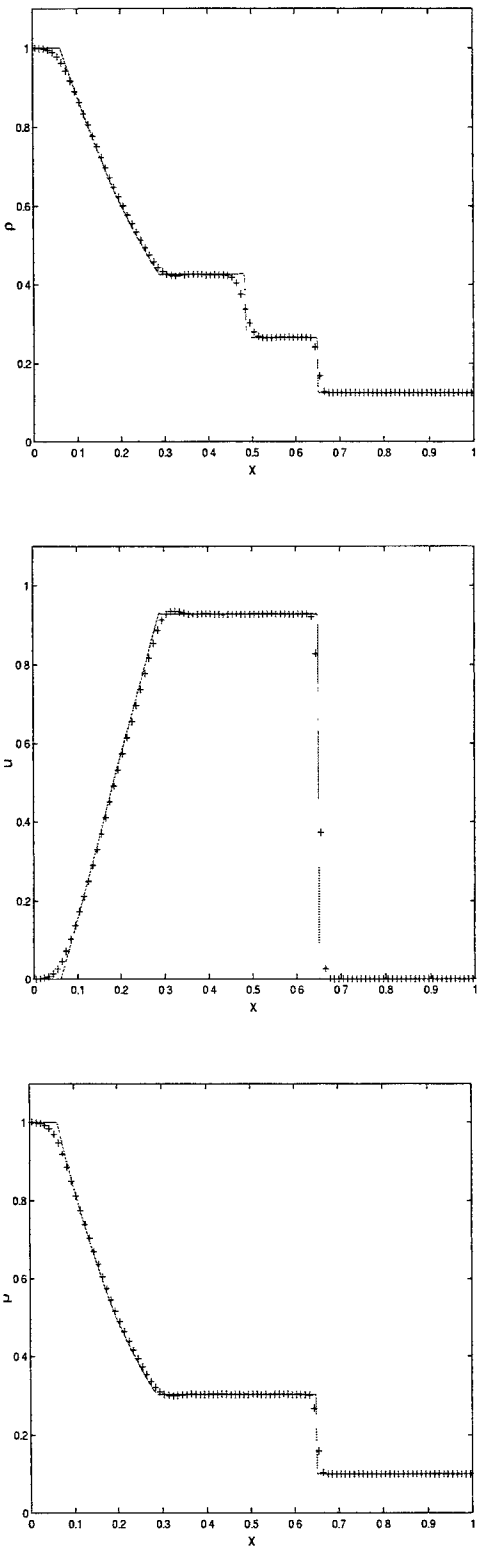

Fig. 1 Numerical solutions of ρ, u and p at $t = 0.2$ are marked by + signs. The solid line in each figure is the fine grid solution generated by the same method and CFL numbers, and 1000 mesh points.

the stiffened gas equation of state

$$\rho e = \frac{p + \gamma p_\infty}{\gamma - 1}. \tag{2.14}$$

As before, γ is the usual ratio of specific heats. p_∞ is a prescribed pressure-like constant. The material parameters γ, p_∞ from laboratory experiments to describe material property of interests. See [3, 7] in this aspect. Following Test 1 in [14], we take $\gamma = 7.15$ and $p_\infty = 300.0\ MPa$ and

$$(\rho, u, p)_L = (1100, 500, 5000),$$

$$(\rho, u, p)_R = (1000, 0, 0.1), \tag{2.15}$$

separated along $x = 0.5$. The units in (2.15) for ρ, u, and p are kgm^{-3}, ms^{-1} and MPa. In the numerical test below, the computational domain is [0, 1] and set $\Delta x = 0.01$. At both ends of the computational domain, the nonreflecting boundary conditions are employed. Time step is determined same as in Example 2.1, except that the sound speed a is now given by $a^2 = \gamma(p + p_\infty)/\rho$. We set $C_{cfl} = 0.8$. At $t = 0.00075$, the resulting profiles of ρ, u, p and e are displayed below in Figure 2.

It is clear that the result in Figure 2 given by the MUSCL type central scheme is significantly better than those given in [14], using the Godunov method and Riemann solvers proposed by Toro. Although the resolution of nonlinear waves given here is not as sharp as what Toro did using his weighted average flux (WAF) method and Riemann solvers, the MUSCL type central scheme is flexible and easy to program as compared to Toro's Riemann-solver based methods. The only difference of the computer programs of the two examples presented here is the pressure is determined differently. Furthermore, test results on speed of execution given in [12] shows that, as compared to traditional Riemann-solver-based methods, the MUSCL type central scheme is significantly faster. In the next section, we will further exploit the flexibility of MUSCL type central scheme and apply it in multicomponent flow computations.

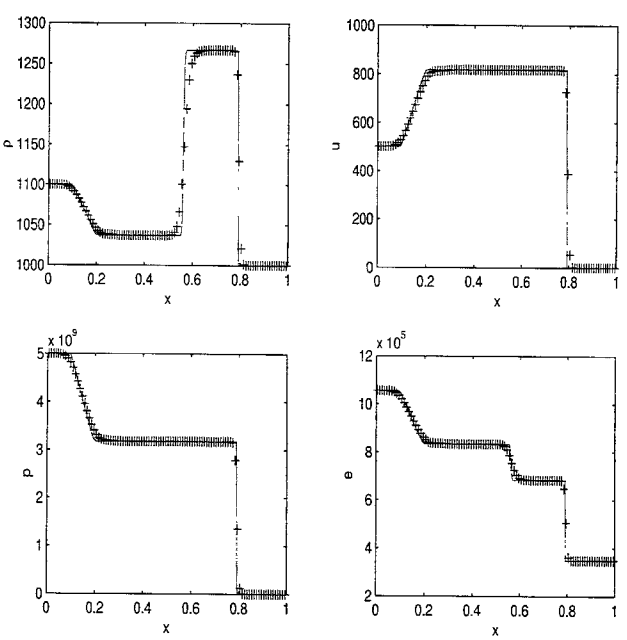

Fig. 2 Numerical solutions of ρ (upper left), u (upper right), p (lower left) and e (lower right) at $t = 0.00075$ are marked by + signs. The solid line in each figure is the fine grid solution generated by the same method and CFL numbers, and 1000 mesh points.

III. Central Schemes for Advection Equations.

In this section, we give a central scheme for solving variable coefficient advection equations. Numerical test on the performance of the resulting central scheme is also given.

A. Numerical schemes

Consider the advection equation

$$U_t + A(x)U_x = 0. \tag{3.1}$$

The first order central scheme that we begin with is chosen to be the arithmetic average of the Lax-Friedrichs scheme

$$U_j^{n+1} = \frac{1}{2}(U_{j+1}^n + U_{j-1}^n) - \frac{\Delta t}{2\Delta x} A_j (U_{j+1}^n + U_{j-1}^n) \tag{3.2}$$

and the Lax-Wendroff scheme

$$\begin{aligned} U_j^{n+1} = U_j^n &- \frac{\Delta t}{2\Delta x} A_j (U_{j+1}^n + U_{j-1}^n) \\ &+ \frac{\Delta t^2}{2\Delta x^2} [A_{j+1/2}(U_{j+1}^n - U_j^n) \\ &- A_{j-1/2}(U_j^n - U_{j-1}^n)]. \end{aligned} \tag{3.3}$$

Take

$$F_j^+ = \frac{1}{2} A_j (U_j^n + U_{j+1}^n) + \frac{\Delta x}{2\Delta t}(U_j^n - U_{j+1}^n), \tag{3.4}$$

$$F_j^- = \frac{1}{2} A_j (U_{j-1}^n + U_j^n) + \frac{\Delta x}{2\Delta t}(U_{j-1}^n - U_j^n), \tag{3.5}$$

$$U_{j+1/2}^{RI} = \frac{1}{2}(U_j^n + U_{j+1}^n) - \frac{\Delta t}{2\Delta x} A_{j+1/2}(U_{j+1}^n - U_j^n). \tag{3.6}$$

Here, in (3.6), we set

$$A_{j+1/2} = \frac{1}{2}(A_j + A_{j+1})$$

Then (3.2) and (3.3) can rewritten as

$$U_j^{n+1} = U_j^n - \frac{\Delta t}{\Delta x}(F_j^+ - F_j^-). \tag{3.7}$$

and

$$U_j^{n+1} = U_j^n - \frac{\Delta t}{\Delta x}A_j(U_{j+1/2}^{RI} - U_{j-1/2}^{RI}) \tag{3.8}$$

respectively. Above the first order solver for (3.1) is referred to as the primitive FORCE scheme and can be implemented by the following steps.

Step 1. In each cell $[x_{j-1/2}, x_{j+1/2}]$, set

$$U_j^{n+1} := U_j^n \tag{3.9}$$

Step 2. At each interface $x = x_{j+1/2}$, set

$$U_j^{n+1} := U_j^{n+1} - \frac{\Delta t}{\Delta x}(F_j^+ + A_j U_{j+1/2}^{RI}), \tag{3.10}$$

$$U_{j+1}^{n+1} := U_{j+1}^{n+1} + \frac{\Delta t}{\Delta x}(F_{j+1}^- + A_{j+1} U_{j+1/2}^{RI}). \tag{3.11}$$

Now we proceed as is usually done in type schemes to sharpen the resolution of the primitive FORCE scheme. In each cell $[x_{j-1/2}, x_{j+1/2}]$, boundary extrapolated values $U_j^{\pm}$ are evolved by half a time step by

$$\bar{U}_j^+ = U_j^+ - \frac{\Delta t}{2}A_j(U_j^+ - U_j^-)$$

$$\bar{U}_j^- = U_j^- - \frac{\Delta t}{2}A_j(U_j^+ - U_j^-). \tag{3.12}$$

Finally, we replace cell averages U_j^n, U_{j+1}^n with $\bar{U}_j^+$ and $\bar{U}_{j+1}^-$ in (3.4), (3.6) and cell averages U_{j-1}^n, U_j^n with $\bar{U}_{j-1}^+$, $\bar{U}_j^-$ in (3.5). We call the resulting high resolution method as the high resolution primitive FORCE scheme for advection equation (3.1). As a direct consequence of the Lax-Friedrichs scheme (3.2) and the Lax-Wendroff scheme (3.3), in scalar equations, we can choose CFL number

$$C_{cfl} = \max_x |A(x)| \frac{\Delta t}{\Delta x} \tag{3.13}$$

up to 1.

B. Numerical Test

Example 3.1 We now apply the primitive FORCE scheme and its high resolution extension to solve the advection equation

$$u_t + \frac{1}{4}xu_x = 0 \tag{3.14}$$

along with the initial condition

$$u(x, 0) = \begin{cases} 1, & x < 0 \\ 0, & x > 0. \end{cases}$$

The computational domain is chosen to be [0, 2], with nonreflecting boundary conditions applied at both end. We use 100 mesh points and CFL number $C_{cfl} = .8$. The numerical solution at $t = 1.5$ is plotted in Figure 3.

Clearly, in Figure 3, the result of the high resolution primitive FORCE scheme improve the first order one significantly. No spurious oscillation is observed in the computational domain. In the following section, the high resolution primitive FORCE scheme will be applied to solve the governing equation for the volume-fraction in two phase flow computation, which appear in the form of

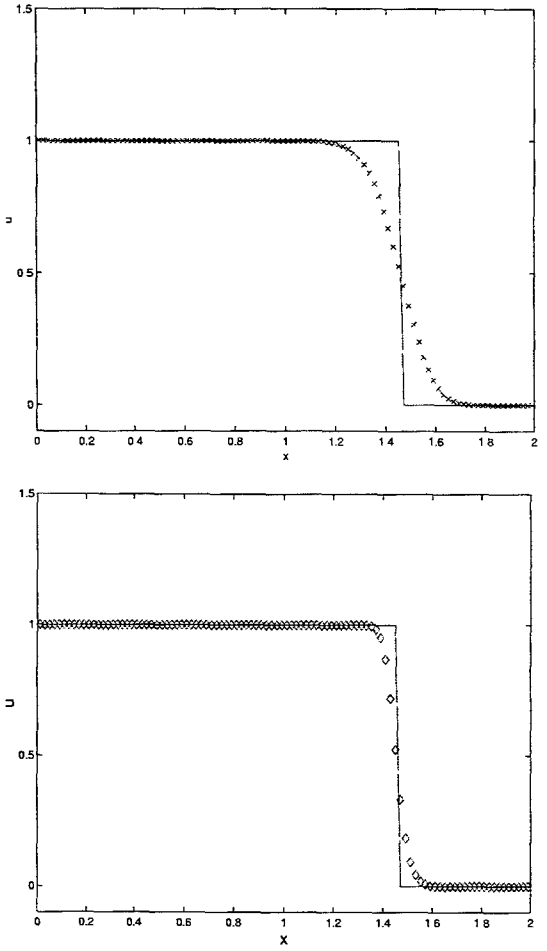

Fig. 3 Numerical solution of (3.14) at $t = 1.5$ generated by the first order FORCE scheme is marked by × signs and the one generated by high resolution primitive FORCES scheme is marked by diamonds. The solid line in each graph denotes the fine grid solution using the same method and CFL numbers, with 1000 mesh points.

advection equation (3.1) with $A(x)$ equal to the velocity field u of the flow.

IV. One-dimensional multicomponent flows

A. Numerical scheme

In this section, we develop multicomponent flow algorithm based on MUSCL type central scheme to simulate the motion of a mixture of fluid governed by the Euler equations (2.11) and the stiffened gas equation of state (2.14). For simplicity, we will assume that there are only two kinds of fluid in the mixture, each has its only set of material parameters $\gamma^{(i)}$ and $p_\infty^{(i)}$, $i = 1, 2$. We adopt the volume-fraction model given in [10] to describe the motion of the mixture of fluids. The governing equations are

$$\begin{aligned}
&\frac{\partial}{\partial t}\rho + \frac{\partial}{\partial x}(\rho u) = 0,\\
&\frac{\partial}{\partial t}(\rho u) + \frac{\partial}{\partial x}(\rho u^2 + p) = 0,\\
&\frac{\partial}{\partial t}E + \frac{\partial}{\partial x}[u(E+p)] = 0,\\
&\frac{\partial}{\partial t}Z + u\frac{\partial}{\partial x}Z = 0.
\end{aligned} \tag{4.1}$$

Here the variable Z is the volume-fraction function of fluid 1. To find the pressure p of the mixture in a consistent manner, we follow Shyue's approach and set

$$\begin{aligned}
&\frac{1}{\gamma-1} = \frac{Z}{\gamma^{(1)}-1} + \frac{1-Z}{\gamma^{(2)}-1},\\
&p_\infty = \left(\frac{Z\gamma^{(1)}p_\infty^{(1)}}{\gamma^{(1)}-1} + \frac{(1-Z)\gamma^{(2)}p_\infty^{(2)}}{\gamma^{(2)}-1}\right)\\
&\quad\cdot\left(1 + \frac{Z}{\gamma^{(1)}-1} + \frac{1-Z}{\gamma^{(2)}-1}\right)^{-1}.
\end{aligned} \tag{4.2}$$

The resulting γ and p_∞ of (4.2) are then substitute into (2.14) to give pressure p. See [10] fot the details of the volume-fraction model for multicomponent flows of stiffened gases.

Our algorithm for solving (4.1) consists of applying the MUSCL type central scheme in §2 and the high resolution primitive FORCE scheme in §3 to solve the Euler equations and the advection equations for volume-fraction function Z. At $t = t_n$, piecewise linear approximations to ρ, ρu, E and Z are constructed and are then used to find their corresponding boundary extrapolated values. Then the boundary extrapolated values of Z are used to determined the boundary extrapolated values for the material parameters γ and p_∞ and also the boundary extrapolated values for pressure. With the boundary extrapolated values of pressure available, we can now evolve the boundary extrapolated values of the conserved variables $U = (\rho, \rho u, E)^T$ by half a time step to $\bar{U}_j^{\pm}$, using (2.4) and flux function $F(U) = (\rho u, \rho u^2+p, u(E+p))^T$. Here T refers to transposes of matrices. The boundary extrapolated values of Z are evolved by half a time step to $\bar{Z}_j^{\pm}$ using (3.12). Let $Z_{j+1/2}^*$ be the outcome of substituting $\bar{Z}_j^+$ and $\bar{Z}_{j+1}$ into (3.6). The value $Z_{j+1/2}^*$ is then substituted into (4.2) to determine the correct material parameters γ and p_∞ to be used in the evaluation of the numerical flux function of MUSCL type central scheme for Euler equations. What remains is to apply the high resolution primitive FORCE scheme to advance Z and the MUSCL type central scheme to update the conserved variables to time t_{n+1}. The effectiveness of the method described here will be tested in what follows.

B. Numerical tests

In the tests below, the time step is determined by setting CFL number $C_{cfl} = 0.8$. See (2.13) for the definition of C_{cfl}. The nonreflecting boundary conditions are applied at both ends of the computational domain.

Example 4.1 We begin by considering an interface problem in which the solution is a single contact discontinuity. At $t = 0$, we consider a polytropic gas has constant states

$$(\rho, u, p, \gamma, p_\infty)_L = (1, 1, 1, 1.4, 0)$$

and

$$(\rho, u, p, \gamma, p_\infty)_R = (0.125, 1, 1, 1.2, 0)$$

separated by $x = 0.2$. In the computation, we use 100 mesh points. The profiles of ρe, u, p and Z at $t = 0.12$ are plotted in Figure 4.

It is clear that u and p remain in equilibrium across the interface within machine accuracy; no $O(1)$ spurious oscillations are seen near the interface as those mentioned in [1, 5, 6, 10].

Example 4.2 Next we assume that the initial data consists of a stiffened gas on the left with

$$(\rho, u, p, \gamma, p_\infty)_L = (10^3, 0, 10^9, 4.4, 6\times10^8)$$

is separated from a gas on the right with

$$(\rho, u, p, \gamma, p_\infty)_R = (50, 0, 10^5, 1.4, 0)$$

along $x = 0.7$. This test can be regarded, initially, as a liquid on the left is separated from a polytropic gas on the

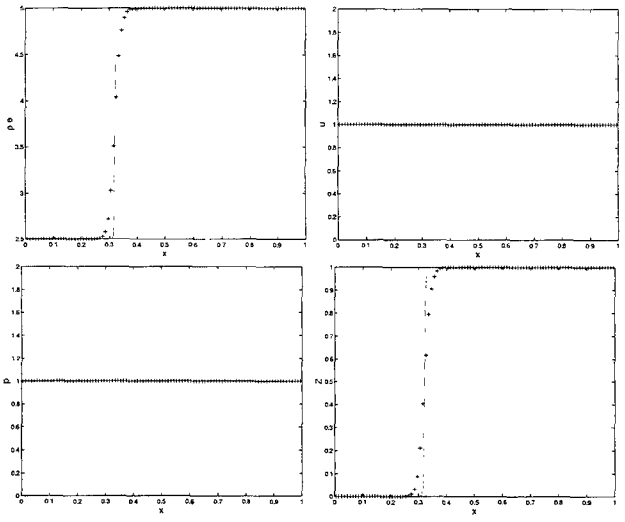

Fig. 4 Numerical solutions of ρe, u, p and Z at $t = 0.12$ are marked by + signs. The solid line in each figure is the fine grid solution generated by the same method and CFL numbers, and 1000 mesh points.

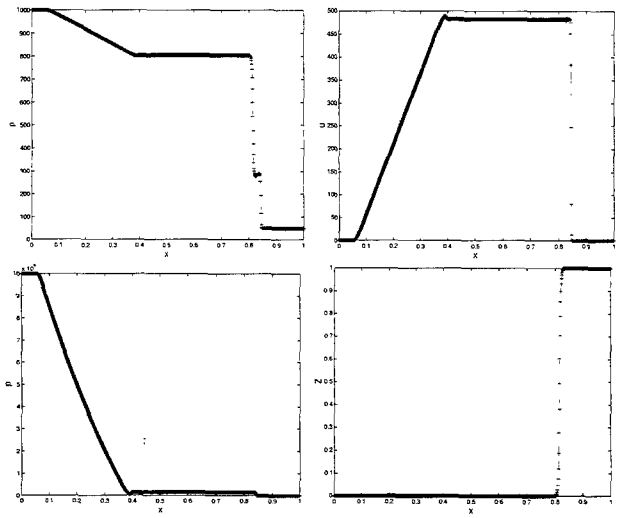

Fig. 5 Numerical solutions of ρ, u, p and Z at $t = 0.00024$ are marked by + signs. The solid line in each figure is the fine grid solution generated by the same method and CFL numbers, and 1000 mesh points.

right by a membrane. Breaking the membrane will result in a left-going rarefaction wave, a right-going contact discontinuity and a shock wave. In the computation, 200 mesh points are used. See Figure 5 for the resulting profiles of ρ, u, p and Z at $t = 0.00024$.

In Figure 5, the profile of u has a over-shoot in the region between 0.3 and 0.4, where the rarefaction wave is connected to a flat region. This situation is caused by MUSCL type central scheme itself. Similar phenomenon is observed in [12] and has nothing to do with updating the pressure in a non-conservative way.

Example 4.3 The third example is a shock-contact interaction problem used in which the interface is hit by a shock wave coming from the heavy-fluid region. The initial data is

$$(\rho, u, p, \gamma, p_\infty)_L = (1, 0, 1, 1.4, 0), \quad x<0.5,$$

$$(\rho, u, p, \gamma, p_\infty)_M = (5, 0, 1, 4, 1), \quad 0.5<x<0.6,$$

$$(\rho, u, p, \gamma, p_\infty)_R = (7.093, -0.7288, 10, 4, 1), \quad x>0.6.$$

At $t = 0$, there is a stationary interface at $x = 0.5$ separating a gas on the left from the stiffened gas on the right. Also, there is a shock at $x = 0.6$, moving from right to left. Once the shock hits the stationary contact discontinuity, a right-going rarefaction, a left-going shock and a contact discontinuity are generated. Profiles of ρe, u and p at $t = 0.2$ are given below in Figure 6 using 200 mesh points.

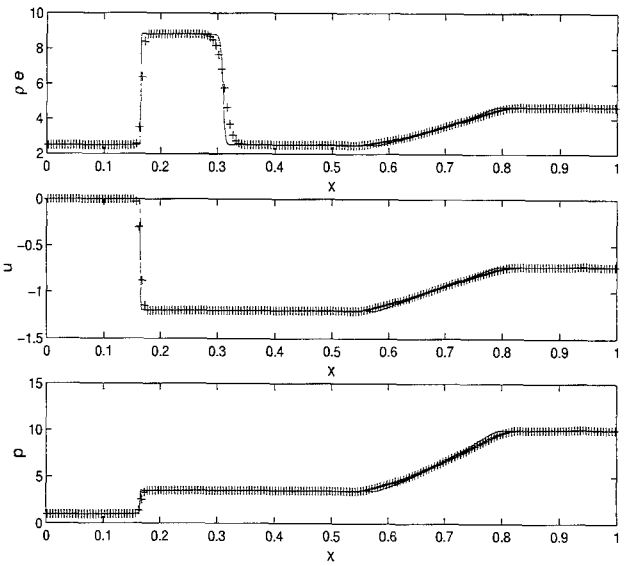

Fig. 6 The profiles of re, u and p at t = 0.2 using 200 mesh points are marked by + signs. The solid lines are the plots of the fine grid solutions using 2000 mesh points.

From Figure 6, we can see that the shock, contact discontinuity and rarefaction wave are located correctly. The result given here matches well with those produced by Shyue in [10] using the Riemann-solver-based wave propagation method.

V. Conclusions

The most attractive feature of MUSCL type central scheme is that it is Riemann-solver-free. Not only can it be executed faster than tradtional Riemann-solver-based methods, it can be applied to a wide range of applications with only minor changes in the computer code. As is demonstrated in §2, MUSCL type central scheme can be used to solve single-component compressible Euler equations with polytropic gas equation of state or stiffened gas equation of state. The Riemann-solver-free feature of MUSCL type central scheme is further exploited in §4 to develop a volume-fraction algorithm for multicomponent flows of stiffened gases. The numerical tests we conducted show that the method proposed in this paper is effective and is capable of eliminating spurious oscillations in velocity and pressure fields across material interfaces.

References

1. R. Abgrall, How to Prevent Pressure Oscillations in Multicomponent Flow Calculations: A Quasi conservative Approach, J. Comput. Phys., 125 (1996), pp. 150-160.
2. A. Harten and S. Osher, Uniformly High Order Accurate Non-oscillatory Scheme I, SINUM, 24(1982), 229-309.
3. K.S. Holian, T-4 Handbook of Material Properties Data Bases, Tech. Rep. LS-10160-MS, Los Alamos National Laboratory, Los Alamos, NM, 1971.
4. G.S. Jiang and Eitan Tadmor, Non-oscillatory Central Schemes for Multidimensional Hyperbolic Conservation Laws, SIAM J. Sci. Comput., 19(1998), pp. 1892-1917.
5. S. Karni, Multicomponent Flow Calculations by a Consistent Primitive algorithm, J. Comput. Phys, 112(1994), pp. 31-43.
6. S. Karni, Hybrid Multifluid Algorithms, SIAM J. Sci. Comput. 17(1996), pp. 1019-1039.
7. S.P. Marsh, LASL Shock Hugoniot Data, Univ. California Press, Berkeley, 1980.
8. H. Nessyahu and E. Tadmor, Non-oscillatory Central Differencing for Hyperbolic Conservation Laws. J. Comput. Phys., 87(1990), pp. 408-463.
9. R. Saurel and R. Abgrall, A Simple Method for Compressible Multifluid Flows, SIAM J. Sci. Comput., 21(1999), pp. 1115-1145.
10. K.M. Shyue, An Efficient Shock-Capturing Algorithm for Compressible Multicomponent Problems, J. Comput. Phys., 142(1998), pp. 208-242.
11. K.M. Shyue, A Volume-Of-Fluid Type Algorithm for Compressible Two-Phase Flow Flows, in Proc. 7th Intl. Conf. Hyperbolic Problems, edited by M. Fey and R. Jetsch (Birkäuser, Basel, 1998), pp. 895-904.
12. T.Y. Sun, Multidimensional MUSCL Type Central Schemes, submitted.
13. E.F. Toro, Riemann Solvers and Numerical Methods for Fluid Dynamics : a practical introduction, Springer-Verlag, Berlin, 1997.
14. E.F. Toro, On Riemann Solvers For Compressible Liquids, Int. J. Num. Meth. Fluids, 28(1998), pp. 395-418.
15. E.F. Toro, Centred TVD Schemes for Hyperbolic Conservation Laws, IMA J. Numer. Ananl., 20(2000), pp. 47-79.

使用 MUSCL 型中央差分法計算多成份流

孫 天 佑　徐 貞 慈
中原大學數學研究所
台灣省中壢市普仁 22 號

摘 要

在本文中，我們經由數值實驗証明使用 MUSCL 型中央差分法與黎曼問題無關的特性，發展單一成份及多成份，使用 stiffened gas 狀態方程式的可壓縮性 Euler方程組數值方法。在本文架構下，在多成份流計算中，針對狀態方程式設計適當的黎曼問題解法的瓶頸，已不復存在。

關鍵詞：可壓縮性 Euler 方程組，多成份流，MUSCL 型中央差分法，黎曼問題解法，stiffened gas 狀態方程式。